

Opacity data for HCN and HNC from a new *ab initio* linelist.

Gregory J. Harris, Oleg L. Polyansky¹ and Jonathan Tennyson².

Department of Physics and Astronomy, University College London, London, WC1E 6BT, UK.

ABSTRACT

A new extensive *ab initio* rotation vibration HCN/HNC linelist is presented. The linelist contains, rotation vibration energy levels, line frequencies and line strengths for transitions between states with energy less than 18 000 cm⁻¹ and with $J \leq 60$. This linelist greatly improves the quality and range of HCN/HNC data available. It is presently the most extensive and most accurate *ab initio* HCN/HNC linelist in existence. It is hoped that this data set will be used in models of C-star atmospheres and elsewhere.

1. Introduction.

HCN and HNC are important molecules throughout astronomy, for example HCN has been observed in comets (Huebner et al. 1974; Irvine et al. 1996), planetary atmospheres (Hidayat et al. 1997), molecular clouds (Hatchell et al. 1998; Hirota et al. 1998), carbon star atmospheres (Aoki et al. 1998, 1999; Bieging et al. 2000) and circumstellar masers (Bieging 2001). In fact, prior to its detection in the interstellar medium in 1971 by the radio astronomers Snyder and Buhl (1971, 1972), HNC had been observed in the laboratory only by means of matrix isolation spectroscopy.

Of particular interest to us is the role of HCN in C-star atmospheres. Calculations by Eriksson et al. (1984) and Jørgensen et al. (1985) suggest that the proper detailed treatment of the vibration-rotation spectrum of HCN can have profound effect on the structure of the C-star model atmospheres. Jørgensen et al. (1985) found that including HCN opacity in their model atmospheres caused the atmosphere to expand by a factor of five and lowered the gas pressure of the surface layers by one or two orders of magnitude.

¹Permanent address: Institute of Applied Physics, Russian Academy of Science, Uljanov Street 46, Nizhnii Novgorod, Russia 603024.

²Corresponding Author: j.tennyson@ucl.ac.uk

Several sets of HCN opacity data have been used in model C-star atmospheres. These include the *ab initio* opacity data of Jørgensen et al. (1985), the empirical data of Jørgensen (1990) and the recent linelist of Aoki et al. (1998). The *ab initio* opacity data of Jørgensen et al. (1985) has been recently used by Loidl et al. (1999), in their model C-star atmospheres. It contains band frequencies and intensities for transitions between states with energy less than $10\,000\text{ cm}^{-1}$. The data of Jørgensen (1990) uses the experimental data of Smith et al. (1987, 1989) with empirical estimates of the intensities of the hot bands. This data includes high frequency bands such as the (40^0_0) C-H stretch overtone. Finally the data of Aoki et al. (1998) is based upon experimental data that has become available since the work of Jørgensen (1990). It covers a limited number of bands, the (01^1_0) , (02^0_0) , (100) , (01^1_1) , (100) - (01^1_0) transitions and their hot bands up to $v_2 = 4$.

All data sets cover the most intense HCN transitions which are primarily the C-H stretch and bend fundamentals and some of their hot bands. The effects of these two modes at 3 and $14\ \mu\text{m}$ are well known. However all these data sets have their weaknesses. The data of Jørgensen (1990) is relatively inaccurate for the hot bands and covers a limited number of bands. The data of Aoki et al. (1998) also cover only a limited number of bands and their hot bands up to $v_2 = 4$. The *ab initio* data of Jørgensen et al. (1985) covers all transitions involving states less than $10\,000\text{ cm}^{-1}$ above the zero point energy, but is inaccurate by today's standards. Furthermore HCN is believed to be an important opacity source in C-stars up to $T_{eff} \sim 2800\text{ K}$ (Eriksson et al. 1984). At these high temperatures states with energy greater than $10\,000\text{ cm}^{-1}$ may contribute significantly to the overall opacity. Finally HNC has been neglected by all workers to date. In thermodynamic equilibrium, the HNC/HCN ratio for $T=2000$ to 4000 K is between 0.05 and 0.34 (Barber et al. 2002). The transitions of HNC are considerably stronger than comparable transitions of HCN, which increases the likelihood that HNC will have a significant effect on opacity.

To increase the amount of HCN and HNC data available and to fill in the gaps in the existing data, we have calculated a new extensive HCN/HNC linelist. This linelist contains rotation vibration energy levels, line frequencies and line strengths for transitions involving states with energy less than $18\,000\text{ cm}^{-1}$ and with values of the rotational quantum number, J , of $J \leq 60$.

In section 2 the calculation of the linelist is discussed, in section 3 the results of the calculation are presented. Finally in section 5 we discuss the results and conclude.

2. Calculation.

Querci and Querci (1970) claimed to detect the (40^0_0) HCN stretching overtone at 791 nm in the atmosphere of the C-star UU Aur. Later Giguere (1973) tentatively identified the (30^0_0) HCN stretching overtone at 1 μm in the same star. However, using a new linelist based on experimental data Jørgensen (1990) disputed that any bands beyond 1.5 μm could be observed in C-star atmospheres. Therefore the aim of this work is to compute the HCN and HNC transitions, including hot bands contributing significantly, longwards of 1.5 μm . To give an accurate value for the band intensity and the distribution of the intensity across the band, the data must extend to a high value of J . Such that for a given band, transitions to and from the highest value of J have only a fraction of the peak line intensity of band. As a result we have extended our linelist to $J \leq 60$. At $T=3000$ K with energy levels less than 18000 cm^{-1} and $J \leq 60$, the rotational vibrational partition function is calculated to be 35653. This is 93 % of the rotationally converged value of 38405, reported in a forthcoming paper (Barber et al. 2002). This gives an indication that the linelist reported here accounts for approximately 93 % of the opacity of HCN/HNC at $T=3000$ K.

The accuracy of the nuclear motion calculation is dependent upon the accuracy of the potential energy surface (PES) and dipole moment surface (DMS) used in the calculation. Therefore it is desirable to use the most accurate PES and DMS available. There are currently three *ab initio* semi-global HCN/HNC PES available these are the ANO/CCSD(T) PES of Bowman et al. (1993), the PES of Varandas and Rodrigues (1997) and the VQZANO+ PES covered in our earlier paper van Mourik et al. (2001). Of these surfaces the VQZANO+ surface uses the largest electronic basis set. As a result, in general, the band origins and intensities calculated with the VQZANO+ surface reproduce more closely the laboratory data than do those calculated with either of the other two semi-global PES, see van Mourik et al. (2001). This surface is also capable of reproducing quite subtle effects observed in laboratory experiments, see Harris et al. (2002). Thus for the calculations performed here we use the VQZANO+ PES.

The *ab initio* VQZANO+ PES simultaneously fits 1527 ANO/CCSD(T) points calculated by Bowman et al. (1993) with 242 points calculated at the higher cc-pCVQZ/CCSD(T) level. The surface is morphed with 17 aug-cc-pCVQZ/CCSD(T) points calculated in the HNC region of the PES, to improve the representation of the HNC part of the surface. To improve the rotational representation the VQZANO+ surface is also adjusted to coincide with three cc-pCV5Z/CCSD(T) points calculated at the critical points of the HCN/HNC system. The VQZANO+ PES includes relativistic and adiabatic corrections, which are often neglected when constructing an *ab initio* PES.

There are three semi-global dipole moment surfaces (DMS) available these are the

TZP/AQCC DMS of Jakubetz and Lan (1997), the aug-cc-pCVTZ/CCSD(T) DMS of Bowman et al. (2001) and the cc-pCVQZ/CCSD(T) DMS of van Mourik et al. (2001). The DMS of Jakubetz and Lan (1997) was calculated with the smallest basis of these three DMS, the intensities calculated with it compare with laboratory data far less favourably than do calculations with the DMS of van Mourik et al. (2001), see Harris et al. (2002). The DMS of Bowman et al. (2001), uses fewer points and a smaller basis than the van Mourik et al. (2001) DMS. The van Mourik et al. (2001) DMS as a result is the best available DMS and the one which will be employed here.

To allow the calculation of HCN and HNC energy levels simultaneously the calculation was performed in Jacobi coordinates. The co-ordinate r was chosen to represent the C-N distance, the R co-ordinate was chosen to be the H to C-N centre of mass distance. Finally the angular co-ordinate γ is the angle between the R and r co-ordinates, the HCN minimum is located at $\gamma = 0$ and the HNC minimum is at $\gamma = \pi$.

Our vibrational, rotational, and transition dipole calculations were performed with the DVR3D program suite (Tennyson et al. 1995), which uses an exact kinetic energy (EKE) operator and a discrete variable representation (DVR) for the vibrational motions. Jacobi coordinates were used with Legendre polynomials to give the angular grid points and Morse oscillator-like functions for the radial grids. 35 grid points were used for the R coordinate, 21 for the r coordinate and 50 for the angular coordinate. This basis was optimised to obtain a balance between the level of convergence and the available computer resources. This basis is large enough to converge all calculations reported here and is the same as used in our previous calculation (Harris et al. 2002). The parameters for the Morse oscillator like basis in the r coordinate are $r_e = 2.3 a_0$, $D_e(r) = 29.0 E_h$ and $\omega_e(r) = 0.0105 E_h$. The parameters for the Morse oscillator like basis in the R coordinate are $R_e = 3.2 a_0$, $D_e(R) = 5.0 E_h$ and $\omega_e(R) = 0.004 E_h$. Where r_e is the equilibrium distance, D_e is the dissociation energy and ω_e is the harmonic frequency, see Tennyson et al. (1995).

The huge number of lines that were calculated required a large amount of processing power. This made it necessary to parallelise the processor intensive routines of the DVR3D codes. The openMP FORTRAN API multiprocessing directives (openMP 2002) with the MIPSpro 7 FORTRAN 90 compiler (MIPSpro, SGI. 2002) on the 'Miracle' 24 processor SGI Origin 2000 computer, were used to perform the parallelisation. The most processor intensive module of the DVR3D suite is DIPOLE3, which calculates dipole transition strengths between states which are not rigorously dipole forbidden. One loop of this module calls a rank 1 matrix update subroutine and consumes 95% of the runtime. By parallelising this loop we were able to reduce the run time by up to a factor of about five when running on eight processors, depending on computer load.

3. Results.

The linelist contains all HCN/HNC transitions involving rotational vibrational energy levels below $18\,000\text{ cm}^{-1}$ and with $J \leq 60$. There are just under 400 million lines and over 168 000 energy levels in the full data set. This is a vast amount of data, that requires a lot of storage space. To fully describe each of the 400 million records requires approximately 20 Gbytes. This size of file is not easily manipulated or ported from machine to machine. Ideally we would like to reduce the overall size of the file and split it into smaller blocks of data which cover specific frequency ranges. The following discussion covers the compact format that has been chosen to store the data.

Each rotational vibrational state is often described by set of quantum numbers, some of which are good quantum numbers and some of which are approximate quantum numbers. The good quantum numbers are the rotational quantum number J , the rotational parity and n , the state number within the J -parity symmetry block. The approximate quantum numbers are the vibrational quantum numbers v_1 , v_2 and v_3 and the vibrational angular momentum l . The good quantum numbers are output from the calculation in conjunction with the energy levels and the wavefunctions. Whereas the approximate quantum numbers are assigned after the calculation.

The 6 integers required to describe the transition are the good quantum numbers of the upper and lower states. The four floating point variables required to describe the transition are the energies of the upper and lower states (E' , E''), the transition frequency (ν) and the Einstein A coefficient (A_{ij}). There are two facts that allow us to store the data in a more compact format. These are:

1. ν can be calculated from E' and E'' .
2. The energy and quantum numbers of each rotational vibrational state are repeated throughout the data file.

Consequently the full transition file can be split into an energy level file and a transition file. The good quantum numbers and energies of each level are stored in the energy level file. Where approximate quantum numbers have been assigned they are also given. An integer flag that identifies the state as HCN, HNC, a delocalised state or unassigned, is also given. Finally each level is given a unique index integer. The index numbers of the upper and lower state and the line strength are stored in the transition file. This is a more efficient way of storing the linelist resulting in nearly a factor of three reduction in file size. Short extracts from the energy level file and the transition file are given in tables 1 and 2.

It is often the case that only a small portion of the spectrum is of interest. It was therefore decided that the file be split into smaller files each with a specific frequency range, thereby allowing only the spectral regions of interest to be downloaded. Further to this the data has also been sorted into frequency order. For the Einstein A coefficient the data beyond the 6th significant figure is meaningless, consequently data is given only to the 6th significant figure. For reasons of compatibility the data has been converted to text format and gzipped.

The Einstein A_{if} coefficient, in s^{-1} is related to the integrated line absorption intensity, I_i , in units of $\text{cm}^{-2} \text{atm}^{-1}$, by:

$$I_i = \frac{3.507293 \times 10^{-6} \times (2J' + 1)}{Q_{vr} \nu^2} \left(\frac{273.15}{T} \right) \exp \left(\frac{-E''}{kT} \right) \left[1 - \exp \left(\frac{-hc\nu}{kT} \right) \right] A_{if} \quad (1)$$

where ν is the wavenumber in cm^{-1} of the line, h is Planck's constant, c is the speed of light, k is Boltzmann's constant, E'' is the energy of the lower rotational-vibrational energy level, T is the temperature and Q_{vr} is the rotational vibrational partition function.

Both the energy level file and the frequency ordered transition files can be retrieved by:

- Anonymous ftp to <ftp.tampa.phys.ucl.ac.uk> and changing to the directory `/pub/astrodata/HCN`,
- or via the TAMPA group web page <http://www.tampa.phys.ucl.ac.uk> and following the links for “Astrodata and Molecular data” then “Astrodata” then “HCN”.

A decompaction code is provided, which is described in the accompanying readme file.

To generate some simple absorption spectra, one needs to obtain k_ν the absorption coefficient or opacity function at frequency or wavenumber ν . The absorption coefficient of the spectrum is given by:

$$k_\nu = \sum_i I_i f_i(\nu - \nu_{0,i}) \quad (2)$$

where $f_i(\nu - \nu_{0,i})$ is the line profile and $\nu_{0,i}$ is the line centre of line i . Once k_ν has been obtained the Lambert-Beer law can be used to generate spectra. The Lambert-Beer law gives the intensity of a beam of radiation passing through a gas of pure HCN, with path length l and pressure p :

$$I_\nu = I_\nu(0) \exp(-k_\nu pl) \quad (3)$$

where $I_\nu(0)$ is the initial intensity of the beam and k_ν is the absorption coefficient or opacity function. The integrated absorption, I_i , of line i is found from the absorption coefficient of

the line, $k_{\nu,i}$, by:

$$I_i = \int_{-\infty}^{+\infty} k_{\nu,i} d\nu \quad (4)$$

The integrated absorption for the complete spectrum is thus:

$$I = \sum_i I_i \quad (5)$$

I is of limited use. Clearly to calculate k_ν one would need to know the line profile of each line and be able to sum over all lines. However, equations 2 and 4 suggest that k_ν for the spectrum in the interval ν to $\nu + \Delta\nu$ can be found more simply. This we do by summing I_i for all lines in the frequency interval $\nu - \nu + \Delta\nu$ and dividing by $\Delta\nu$. This frequency binning method gives an approximate average value for k_ν in the region ν to $\nu + \Delta\nu$. It also has the effect of reducing the resolution of the full spectrum to $\nu/\Delta\nu$. Frequency binned opacity data has been presented by, for example, Schryber et al. (1995) and Neale et al. (1996). This method is adequate to illustrate the usefulness of the linelist and obtain some simple absorption spectra. There are more sophisticated methods for opacity sampling which are beyond the scope of this work.

4. Discussion.

To demonstrate the usefulness of our linelist we now compare our opacity data with observed stellar spectra. The resolving power of the ISO SWS spectrometer in its low resolution mode (SWS01) is about 200 (ISO Data Centre. 2002). This is the resolution at which Aoki et al. (1998) have observed C-star spectra. So for spectra of comparable resolution integrated absorption intensities have been put into bins of 3 cm^{-1} . Figures 1 and 2 show the resulting absorption coefficient (k_ν) in the spectral region of 300 to 1100 cm^{-1} and 1100 to 3900 cm^{-1} at temperatures of 1500, 2000, 2500 and 3000 K. In the 300 to 1100 cm^{-1} interval there are over 73 million lines, the main features are a result of $\Delta v_2 = 1$ HCN and HNC bending fundamentals and hot bands, centred on 715 cm^{-1} and 465 cm^{-1} respectively. In the 1100 to 3900 cm^{-1} frequency interval there are over 165 million lines and there are several strong absorption features. These are the HCN $\Delta v_2 = 2$ overtone and its hot bands at $\sim 1400 \text{ cm}^{-1}$, the HNC CN stretch fundamental and hot bands at $\sim 2000 \text{ cm}^{-1}$, the HCN $(10^0) - (01^10)$ band and its hot bands at $\sim 2600 \text{ cm}^{-1}$, the HCN HC stretch fundamental and hot bands at $\sim 3300 \text{ cm}^{-1}$ and the HNC HN stretch fundamental and hot bands at $\sim 3660 \text{ cm}^{-1}$. The HCN CN fundamental, its hot bands, the $\Delta v_2 = 3$ overtone and hot bands at $\sim 2100 \text{ cm}^{-1}$ are just discernible. As is the Q branch of the $(01^11) - (000)$ band at $\sim 2800 \text{ cm}^{-1}$. In both spectral ranges HNC features contribute significantly to the opacity

and lie in regions where there is little HCN absorption. We have used HCN/HNC partition functions of 3523.9, 8731, 19288 and 38405 at $T=1500, 2000, 2500$ and 3000 K respectively. These are rotationally converged values and will be reported in a forthcoming paper (Barber et al. 2002).

The effect of temperature on opacity is evident in figures 1 and 2. In general, with increasing temperature, the absorption features resulting from strong HCN bands broaden whilst their peak absorption decreases. This is a result of the excited HCN states becoming more populated whilst the population of the HCN ground state decreases. Consequently, and not suprisingly the hot bands become responsible for more absorption as temperature increases. For HNC, as temperature increases the strong HNC features broaden and their peak absorption increases. This is primarily a result of the population of HNC increasing with respect to HCN as temperature increases. The ratio of the intensity of the HCN HC stretch fundamental to the HNC HN stretch fundamental may prove to be a useful tool for obtaining temperature estimates. The temperature dependence of the HNC/HCN ratio will be discussed in detail Barber et al. (2002).

To generate some simple absorption spectra we use the Lambert-Beer law, equation 3. This allows a determination of the transmittance ($I/I(0)$) of the beam, from κ_ν . Figure 3 shows the spectrum generated with our HCN/HNC opacity function, over the wavelength range 2.6 to $8 \mu\text{m}$. This range is comparable to the range over which Aoki et al. (1998) measured the spectra of six C-stars. Most of the main features in the HCN/HNC spectra (fig 3) appear to correlate well with the stellar spectra. For example the $3.2 \mu\text{m}$, $4 \mu\text{m}$ and the $7-8 \mu\text{m}$ features are present in both HCN/HNC and the stellar spectra of (Aoki et al. 1998). The $\sim 5 \mu\text{m}$ HNC CN stretch features present in the HCN/HNC spectrum, may be present in the stellar spectra. However this is difficult to confirm, in the case of the HNC CN stretch feature there is absorption from other molecular species, possibly C_3 (Aoki et al. 1998).

Aoki et al. (1998) have also taken higher resolution spectra of TX-Psc and WZ Cas in the 2.75 to $4.2 \mu\text{m}$ region. They used ISO's SWS06 spectrometer, which has a resolution of around 1500. For comparison with these stellar spectra we have calculated a HCN/HNC spectrum in the same region, see figure 4. To aid the reader we have also plotted the spectrum of WZ Cas taken by Aoki et al. (1998) in figure 4, the stellar spectrum has not been normalised. The 2 major features, at $3.2 \mu\text{m}$ and $4 \mu\text{m}$ of the spectrum of WZ Cas are present in the HCN/HNC spectra. The $4 \mu\text{m}$ feature is attributable to the $(10^00) - (01^10)$ band and its hot bands. The $\sim 2.8 \mu\text{m}$ HNC HN stretch feature present in the HCN/HNC spectrum, may also be present in the stellar spectrum. A more detailed comparison, which could include a proper temperature determination, must await a full stellar model based on

our new data.

The C-star synthetic spectra calculated by Aoki et al. (1998) indicate that the predicted strength of the $4 \mu\text{m}$ absorption feature is particularly sensitivity to the amount of hot band data used. The HCN opacity data used by Aoki et al. (1998) is based upon experimental data, it includes transitions with bend excitations up to $v_2 = 4$. The limited nature of this data resulted in a considerable discrepancy between the synthetic and observed spectra of Aoki et al. (1998). In an attempt to better model this feature Aoki et al. (1998) used an empirical extension to their data to extend it up to hot bands containing $v_2 = 9$. The synthetic spectra calculated with the extended HCN data compares considerably better with the observed spectra. The data used by Aoki et al. (1998) is considerably less extensive than the data presented here. Our data will not suffer from this lack of hot band data. Aoki et al. (1998) identified the Q branch of the $(01^11) - (00^00)$ overtone in the spectrum of WZ Cas. The Q branch of this band is visible in the HCN/HNC spectrum at $\sim 3.55 \mu\text{m}$, but is much less pronounced at than in the model atmosphere spectra of Aoki et al. (1998). The $\sim 2.85 \mu\text{m}$ HNC HN stretch feature present in the HCN/HNC spectrum is perhaps visible in the spectrum of WZ Cas. This is another and possibly the most promising region in which HNC could be looked for in C-stars. If detected the ratio of the peak intensity of the HNC $\Delta v_1 = 1$ bands to the HCN $\Delta v_1 = 1$ bands may prove a useful tool with which to estimate temperature.

5. Conclusion.

The main HCN features in the *ab initio* HCN/HNC spectra presented here are in good qualitative agreement with the HCN features in the C-star spectra observed by Aoki et al. (1998). This shows the usefulness of this new HCN/HNC linelist. The data presented here indicates that if HCN and HNC are in thermodynamic equilibrium, HNC will play a significant role in the opacity of HCN containing C-stars. Possible regions in which HNC might be detected in C-stars has been identified as the regions of the HNC fundamentals at $\sim 2.8 \mu\text{m}$, $\sim 5 \mu\text{m}$ and $\sim 20 \mu\text{m}$. The $\sim 2.8 \mu\text{m}$ feature looks the most promising region in which to observe HNC. If observed, the ratio of the peak intensity of the HNC $\Delta v_1 = 1$ ($\sim 2.8 \mu\text{m}$) absorption feature to the HCN $\Delta v_1 = 1$ ($\sim 3.1 \mu\text{m}$) absorption feature may be a useful tool for obtaining temperature estimates.

In conclusion the linelist presented here is the most extensive HCN/HNC data set in existence. The linelist is more accurate and more extensive than the *ab initio* HCN opacity data of Jørgensen et al. (1985), that is used in the recent model C-star atmospheres of Loidl et al. (1999). It is considerably more extensive than the data of Aoki et al. (1998), which is

based upon experimental data. Therefore the use of the linelist in a full stellar model should result in important effects. This linelist is publicly available for use in stellar atmosphere models and otherwise.

We thank Callum Wright for the great deal of help he provided with computer system issues. We thank Dr. Hugh Jones for extracting the spectrum of WZ Cas from the ISO public archives. We thank the UK Particle Physics and Astronomy Research Council (PPARC) for Ph.D. studentship funding. The calculations reported in this work were carried out on the Miracle 24-processor Origin 2000 supercomputer at the HiPerSPACE computing centre, UCL, which is part funded by PPARC.

REFERENCES

- Aoki, W., Tsuji, T., and Ohnaka, K. 1998, *A & A.*, 340, 222.
- Aoki, W., Tsuji, T., and Ohnaka, K. 1999, *A & A.*, 350, 945.
- Biegging, J. H., Shaked, S., and Gensheimer, P. D. 2000, *ApJ*, 543, 897.
- Biegging, J. H. 2001, *ApJ*, 549, L125.
- Barber, R. J., Harris, G. J., and Tennyson, J. J. *Chem. Phys.* , (TO BE SUBMITTED).
- Bowman, J. M., Gazdy, B., Bentley, J. A., Lee, T. J. and Dateo, C. E. 1993, *J. Chem. Phys.* , 99, 308.
- Bowman, J. M., Irle, S., Morokuma, K., and Wodtke, A. 2001, *J. Chem. Phys.* , 114, 7923.
- Eriksson, K., Gustafsson, B., Jørgensen, U. G., and Nordlund, Å. 1984, *A & A.*, 132, 37.
- Giguere, P. T. 1973, *ApJ*, 186, 585.
- Harris, G. J., Polyansky O. L., and Tennyson, J. 2002, *Spectrochimica Acta Part A.* 58, 673
- Hatchell, J., Millar, T. J., and Rodgers S. D. 1998, *A & A.*, 332, 695.
- Hidayat, T., Marten, A., Bežard, B., Gautier, D., Owen, T., Matthews, H. E., and Paubert, G. 1997, *Icarus*, 126, 170.
- Hirota, T., Yamamoto, S., Mikami, H., and Ohishi, M. 1998, *ApJ*, 503, 717.
- Huebner, W. F., Snyder, L. E., and Buhl, D. 1974, *Icarus*, 23, 580.

Irvine, W. M., BockeleeMorvan, D., Lis, D. C., Matthews, H. E., Biver, N., Crovisier, J., Davies, J. K., Dent, W. R. F., Gautier, D., Godfrey, P. D., Keene, J., Lovell, A. J., Owen, T. C., Phillips, J. G., Rauer, H., Schloerb, F. P., Senay, M., Young, K. 1996, *Nature*, 383, 418.

ISO Data Centre. 2002, <http://isowww.estec.esa.nl>

Jakubetz, W. and Leong Lan, B. 1997, *Chem. Phys.*, 217, 375.

Jørgensen, U. G., Almlöf, J., Gustafsson, B., Larsson, M., and Siegbahn, P. 1985, *J. Chem. Phys.* , 83, 3034.

Jørgensen, U. G. 1990, *A & A.*, 232, 420.

Loidl, R., Höfner, S., Jørgensen, U. G., and Aringer, B. 1999, *A & A.*, 342, 531.

Silicon Graphics Inc. 2002, MIPSpro compilers,
<http://www.sgi.com/developers/devtools/languages/mipspro.html>

Neale, L., Miller, S., and Tennyson, J. 1996, *ApJ*, 464, 516.

openMP consortium. 2002, <http://www.openmp.org>

Querci, M., and Querci, F. 1970, *A & A.*, 9, 1.

J. H. Schryber, S. Miller and J. Tennyson. 1995, *J. Quant. Spectrosc. Rad. Transf.*, 53, 373

Smith, A. M., Jørgensen, U. G., and Lehmann, K. K. 1987, *J. Chem. Phys.* , 87, 5649.

Smith, A. M., Coy, S. L., Klemperer, W. and Lehmann, K. K. 1989, *J. Mol. Specty.* , 134, 134.

Snyder, L. E., and Buhl, D. 1971, *BAAS*, 3, 388.

Snyder, L. E. and Buhl, D. 1972, *Ann. N.Y. Acad. Sci.*, 194, 17.

Tennyson, J., Henderson, J. R., and Fulton, N. G. 1995, *Computer Phys. Comms.*, 86, 175.

van Mourik, T., Harris, G. J., Polyansky, O. L., Tennyson, J., Császár, A. G., and Knowles, P. J. 2001, *J. Chem. Phys.* , 115, 3706.

Varandas, A. J. C., and Rodrigues, S. P. J. 1997, *J. Chem. Phys.* , 106, 9647.

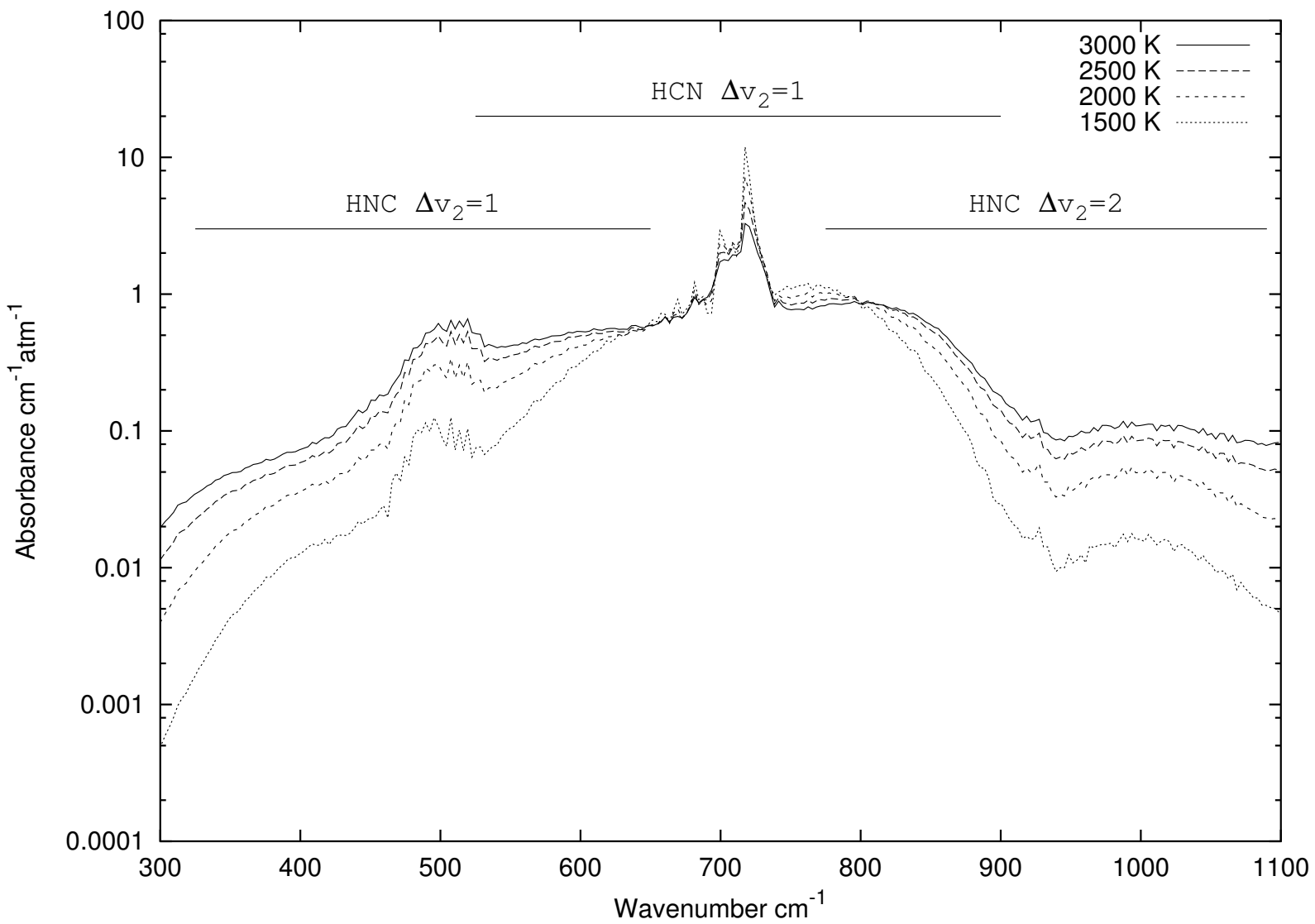


Fig. 1.— The absorption coefficient at $T=1500, 2000, 2500$ and 3000 K at STP, in the region of the HCN and HNC bend fundamentals.

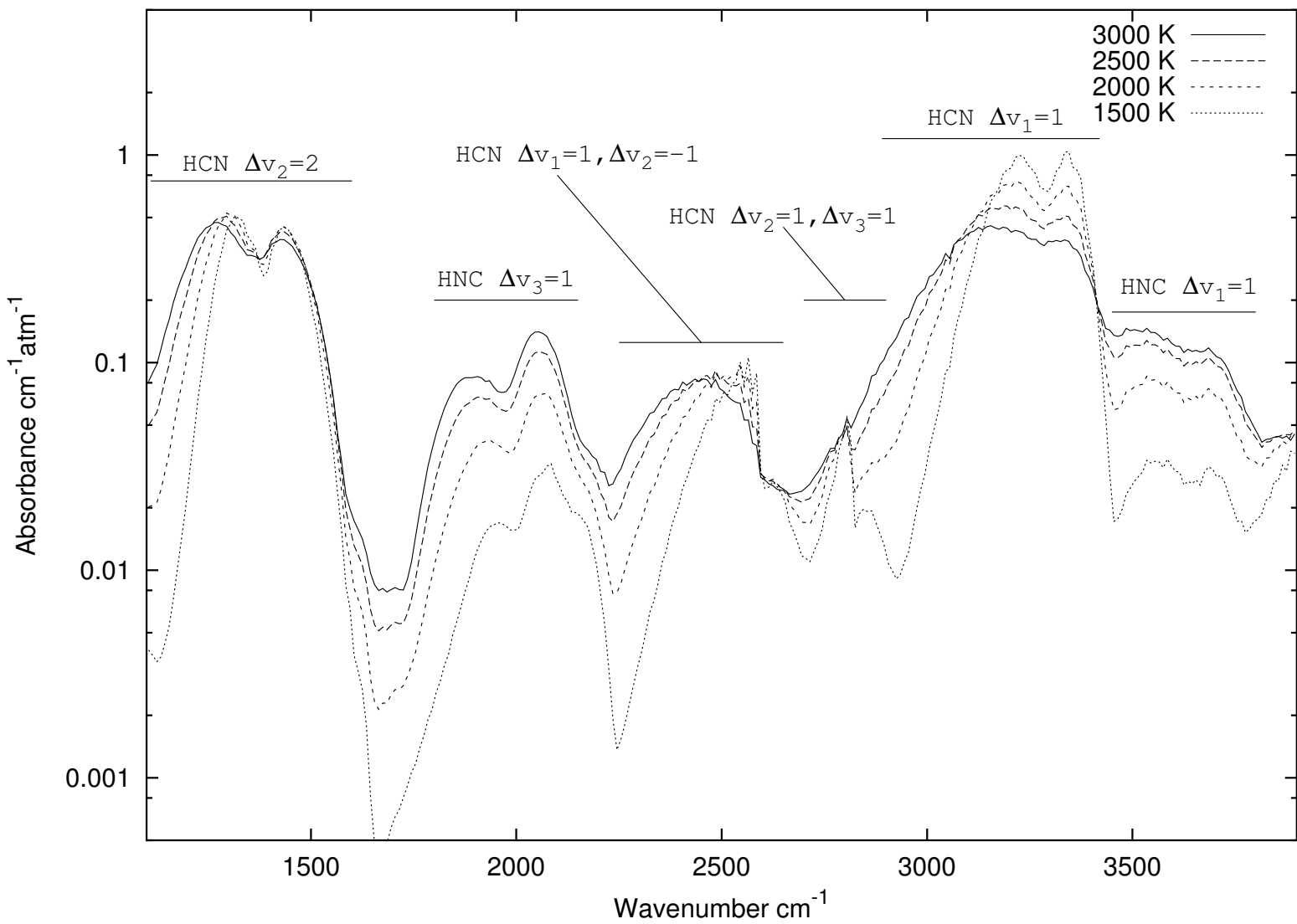


Fig. 2.— The absorption coefficient at $T=1500, 2000, 2500$ and 3000 K at STP, in the region of the HCN and HNC stretch fundamentals.

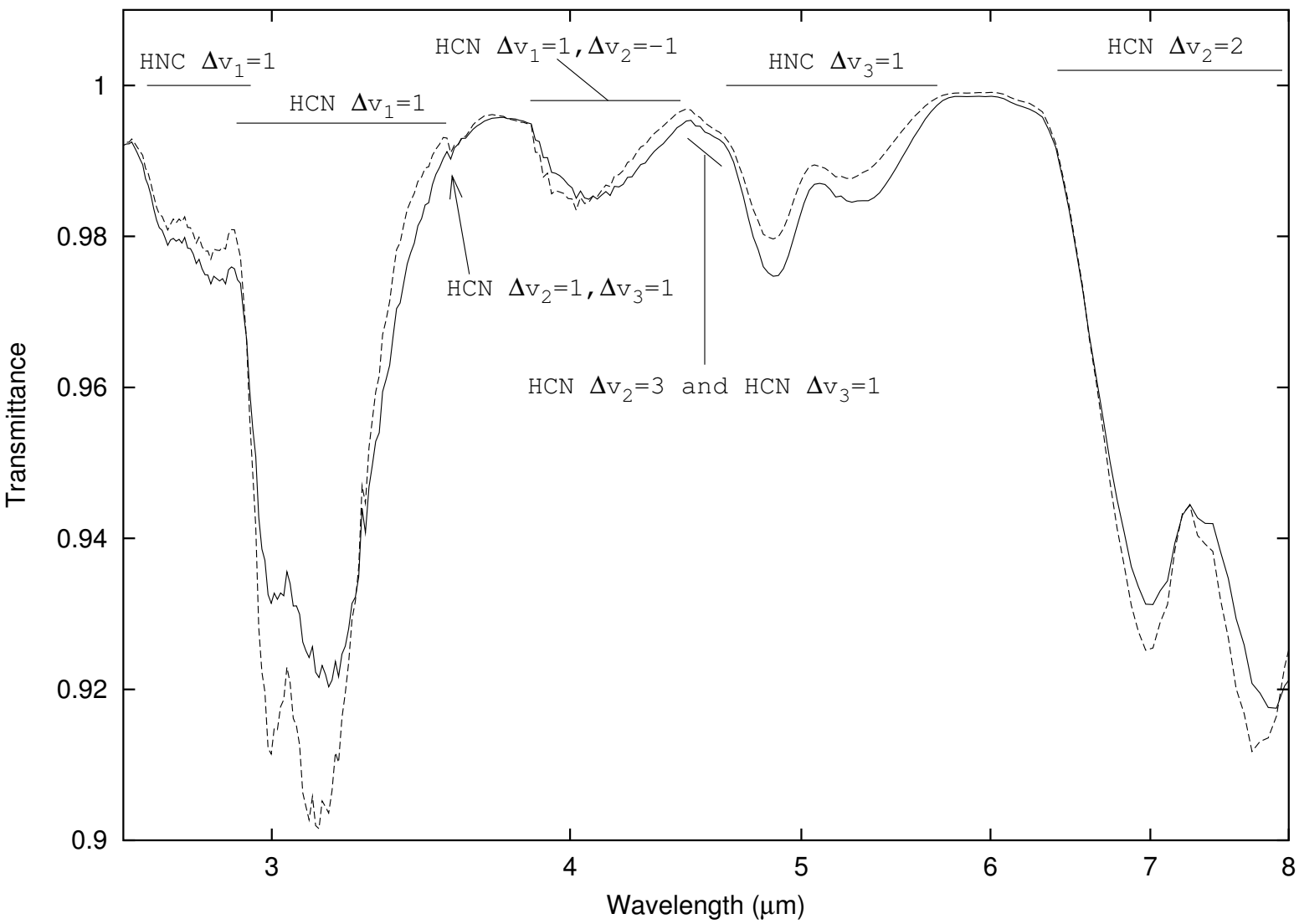


Fig. 3.— Transmittance (I/I_0) using a path length of 2 cm at 1 atmosphere at $T=3000\text{ K}$ solid line and $T=2500\text{ K}$ dashed line. The size of the bins is $\sim 0.01\ \mu\text{m}$.

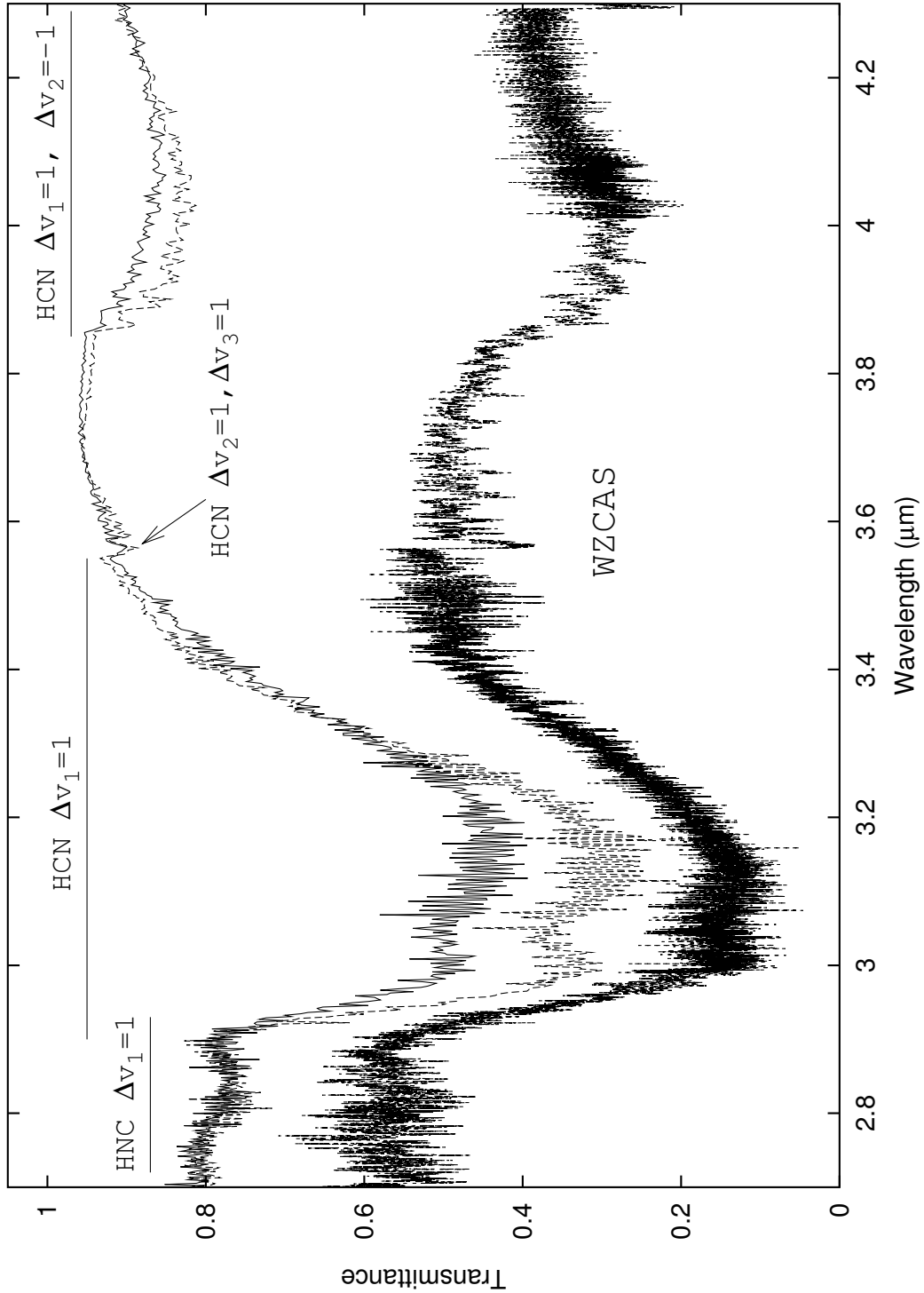


Fig. 4.— Transmittance (I/I_0) using a path length of 20 cm at 1 atmosphere at $T = 3000$ K solid line and $T = 2500$ K dashed line. The wavenumber range selected is in the region of the HCN and HNC stretching fundamentals and the $\Delta v_2 = 2$ overtone. The size of the bins is $\sim 0.002 \mu\text{m}$. The lower spectrum is the unnormalised spectrum of the C-star WZ Cas taken by Aoki et al. (1998). The stellar spectrum is on an arbitrary linear scale with a constant subtracted to stagger the spectra.

Table 1: An extract from the full energy level file.

index	J	p^a	n	E (cm ⁻¹) ^b	i^c	v_1	v_2	l	v_3
1	0	1	1	0.000000	0	0	0	0	0
2	0	1	2	1414.915929	0	0	2	0	0
3	0	1	3	2100.582377	0	0	0	0	1
4	0	1	4	2801.459102	0	0	4	0	0
5	0	1	5	3307.745835	0	1	0	0	0
6	0	1	6	3510.991764	0	0	2	0	1

^aIf $p = 1$ this is an e state, if $p = 0$ this is an f state.

^bThis is the energy of the level relative to the HCN ground state. The zero point energy is 3481.5053 cm⁻¹.

^cThis flag denotes the structure of the molecule in this state. $i = 0$ denotes HCN, $i = 1$ denotes HNC, $i = 2$ denotes a delocalised state and $i = 3$ denotes an unassigned state.

Table 2: An extract from the transition file, upper state is i , lower state is j .

index i	index j	A_{ij} ^a
6530	9178	0.328590D-21
157848	158599	0.354054D-15
19118	15561	0.151754D-16
40575	44648	0.918852D-18
32589	30544	0.113946D-13

^aThis is the Einstein A coefficient, in s⁻¹, of the transition between state i (upper) and state j (lower).